Controlled manipulation of individual vortices in a superconductor

E. W. J. Straver,[1] J. E. Hoffman,[1,2] O. M. Auslaender,[1,a)] D. Rugar,[3] and Kathryn A. Moler[1]
[1]*Departments of Applied Physics and Physics and Geballe Laboratory for Advanced Materials, Stanford University, Stanford, California 94305, USA*
[2]*Department of Physics, Harvard University, Cambridge, Massachusetts 02138, USA*
[3]*IBM Research Division, Almaden Research Center, 650 Harry Road, San Jose, California 95120, USA*

(Received 6 August 2008; accepted 24 September 2008; published online 30 October 2008)

We report controlled local manipulation of single vortices by low temperature magnetic force microscopy in a thin film of superconducting Nb. We are able to position the vortices in arbitrary configurations and to measure the distribution of local depinning forces. This technique opens up possibilities for the characterization and use of vortices in superconductors. © *2008 American Institute of Physics*. [DOI: 10.1063/1.3000963]

Quantized magnetic flux tubes, called vortices, allow superconductivity to survive in high applied magnetic field in type-II superconductors, making them more technologically relevant than type I. Each vortex has a nonsuperconducting core with a radius on the scale of the coherence length ξ and a circulating supercurrent that generates one quantum of magnetic flux, $\Phi_0=h/2e$, over the scale of the London penetration depth λ. Although the paired electrons in a superconductor carry charge without resistance, a current will exert a magnus force on all vortices, which results in dissipation, if any of them move. Vortex motion is both a challenge and an opportunity. The challenge is to understand and reduce uncontrolled vortex motion. A vortex may be pinned in place by colocating its energetically costly nonsuperconducting core with a defect that locally suppresses superconductivity. Decades of materials research have characterized pinning strengths and engineered defects to increase pinning.[1–4] Continued reduction in uncontrolled vortex motion will open up applications both for quiet circuits in sensing and communication and for large currents in high-field magnets and power distribution.

Controlled vortex motion, on the other hand, has great prospects for logic applications and for fundamental science. Collectively controlled vortex motion can serve as a rectifier,[5] a vortex ratchet mechanism can perform clocked logic,[6] and vortices can control spins in an adjacent diluted magnetic semiconductor,[7] while vortices adjacent to an electron gas in a quantum-Hall state may allow the creation of exotic quantum states.[8] A proposed test[9,10] of the long-standing idea that vortices may entangle like polymers[11] requires controlled local manipulation of single vortices. Vortices are of theoretical interest for their own sake,[12,13] as clues to the underlying superconductivity,[14,15] as analogs for interacting bosons,[16] and as model systems for soft condensed matter.[13]

Previous experimental manipulations of single vortices applied relatively delocalized forces[17–21] or did not control the vortex motion.[22,23] Here we demonstrate vortex manipulation with nanoscale control and show that we can quantitatively measure the local depinning force. In magnetic force microscopy (MFM), the sample exerts a measurable force on a cantilever with a sharp magnetic tip, such that scanning the cantilever at a constant height z above the sample provides a map of magnetic features. MFM has been used for a variety of vortex experiments.[22–27] Many experiments image the cantilever deflection, which is proportional to the vertical force F_z. For improved signal-to-noise ratio, we use frequency modulation mode[28] in which the imaging signal is a shift Δf in the cantilever's resonant frequency f_0. The images show the variations in the derivative of F_z, $\partial F_z/\partial z = -2k\Delta f/f_0$, where k is the cantilever's spring constant.[29] We use the lateral component of the force $F_{\mathrm{lat}} \equiv |F_x\hat{x}+F_y\hat{y}|$ to pull or push vortices.

We used a home-built variable-temperature MFM[30] to study a 300 nm thick Nb film sputtered onto a silicon substrate.[31] The midpoint transition temperature is $T_c = 8.6$ K with a transition width $\Delta T_c = 0.6$ K, as measured by magnetic susceptibility, and $\lambda = 90$ nm.[32]

Figure 1 shows controlled vortex manipulation. We cooled the sample to $T=7$ K in an external field of a few Gauss with a polarity giving an attractive tip-vortex force. Figure 1(a) shows a disordered arrangement of vortices pinned in the sample. The lack of observed vortex motion

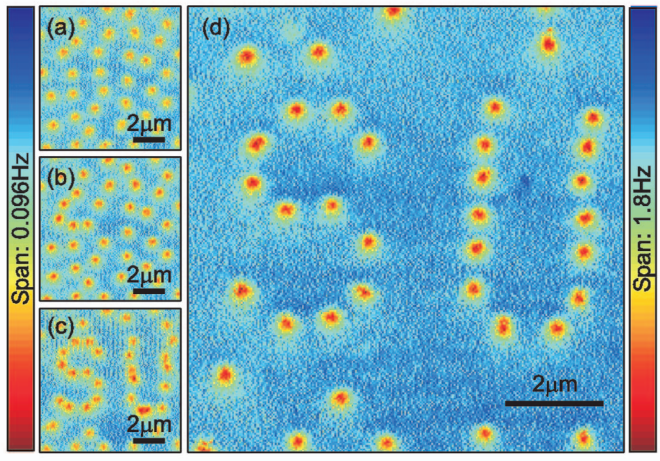

FIG. 1. (Color) Manipulation of vortices to spell SU. Color bars give Δf [left for (a)–(c), right for (d)]. (a) An unmanipulated configuration of pinned vortices after initial cooling to $T=7.0$ K imaged at a scan height $z=300$ nm. [(b)–(c)] Intermediate configurations after manipulation of some vortices in the temperature range 7.0 to 7.2 K, imaged at $z=300$ nm. (d) Final configuration after completing the vortex manipulation at 7.2 K, imaged at $z=120$ nm and $T=5.5$ K for better resolution and stronger pinning.

a)Author to whom correspondence should be addressed. Electronic mail: ophir@stanford.edu.

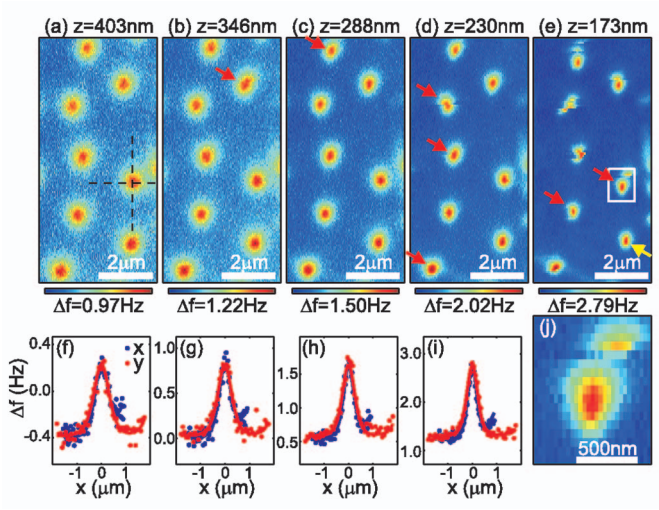

FIG. 2. (Color) Vortices in a Nb film imaged at $T=5.5$ K as a function of decreasing scan height z. [(a)–(e)] Images at five different values of z. Red right arrows indicate vortices depinning for the first time. A single vortex remains unmoved even at the largest applied force in (e) (yellow left arrow). [(f)–(i)] Cross sections along the crosshairs in (a) for the first four z-values. The lines are from the monopole-monopole model. (j) Closeup on the boxed region in (e).

during the scan indicates that at this height of $z=300$ nm we are imaging vortices without depinning them. To move a vortex, we position the cantilever tip over it, reduce the oscillation amplitude, descend to $z\approx 10$ nm, move parallel to the surface, and then withdraw vertically, leaving the vortex at a new location. Some locations require several attempts at different heights or lateral offsets to move the vortex or different pulling directions and slightly elevated temperature to reduce the pinning force. The exact final location of the vortex must depend on the local pinning potential; pinning sites appear to be dense in the Nb film. Images [Figs. 1(b)–1(d)], each taken after several manipulations, show the repositioning of vortices to write SU. This procedure is akin to atom manipulation in scanning tunneling microscopy.[33]

We also quantified the forces required to depin vortices at 5.5 K. Figure 2 shows a series of images, with decreasing z, of eight isolated vortices at a vortex density corresponding to 4 G with a polarity giving repulsive tip-vortex force. As z decreases, the increased $\partial F_z/\partial z$ leads to increased signal strength, while the increasing F_{lat} depins vortices. Vortices at different locations depin at different heights, indicating a distribution of depinning forces. In this case, F_{lat} is weak enough that a depinned vortex simply finds a better pinning site nearby, but we have also applied larger forces to sweep the field of view clean of vortices.

We fit the data in Fig. 2, as well as a second data set of 31 vortices at a vortex density corresponding to 17 G, also at 5.5 K. We model the cantilever tip and each vortex as monopoles.[29] Cuts through the fits are shown in Figs. 2(f)–2(i). The resulting $\max(F_z)$ [Fig. 3(a)] has systematic error bars of less than 50% from the modeling and from the uncertainty in k. These systematic errors do not affect the relative distribution of depinning forces.

Most vortices clearly moved by visual inspection during one or more scans. To quantify our detection threshold, we bootstrap[29,34] the entire eight-vortex data set and one quadrant of the 31-vortex data set.[29] The upper limit to undetected vortex motion at the 95% confidence level δR is shown in Fig. 3(b). The stationary vortex in Fig. 2 did not move by more than 9 nm.

Identifying the z-value at which each vortex moved gives a histogram of vertical depinning forces [Fig. 3(c)] ranging from 12 pN to more than 32 pN. Since it is actually F_{lat} that causes the depinning, we use modeling to estimate it based on the measured $\max(F_z)$. Depending on the model, the ratio between the maximum F_{lat} and the maximum F_z ranges from 0.3 for a pyramidal tip less sharp than ours[35] to $2/3\sqrt{3}\approx 0.38$ in the monopole-monopole model. Using 0.38, the observed lateral depinning force ranges from 4 pN to above 12 pN or, normalized by film thickness, 15–40 pN/μm. This technique could be advanced further by using vertical cantilevers with lower spring constants to directly measure the lateral force.

The manufacturer-specified critical current for similar films is 50 ± 30 mA per transverse micrometer at 4.2 K,[31] equivalent to a depinning force of 104 ± 69 pN. Other single vortex pinning measurements in Nb used a transport current to supply a force[17–20] and various stationary probes to detect

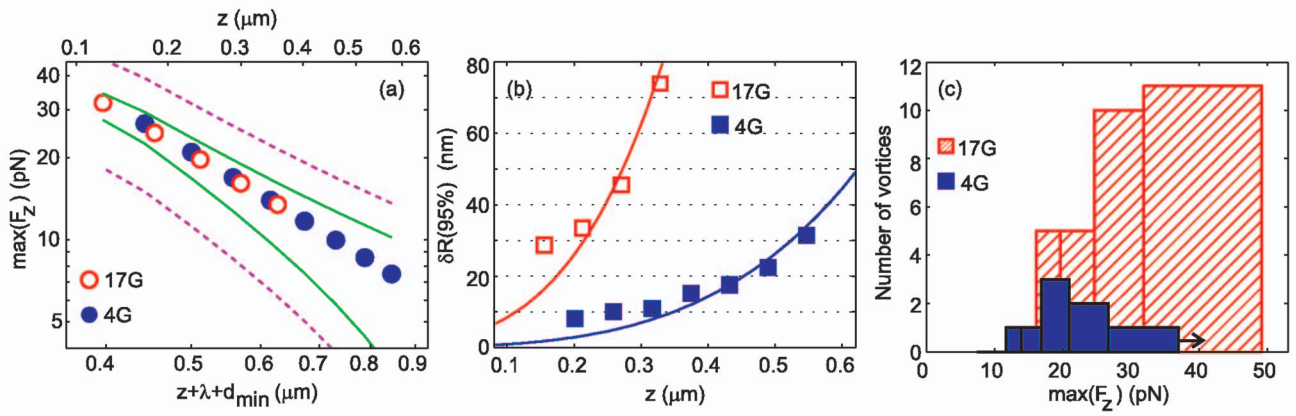

FIG. 3. (Color) (a) Maximum of the vertical force applied to a vortex $\max(F_z)$ as a function of the measured tip-sample separation z and the modeled monopole-monopole separation $z+\lambda+d$ for two data sets taken with the same cantilever. Solid green lines indicate the systematic error associated with modeling the data. Dashed purple lines also include the uncertainty from the cantilever spring constant. (b) The threshold for detecting vortex motion at the 95% confidence level. The 4 G data set has better resolution because the data were less noisy. The curves are from the monopole-monopole model.[29] (c) Histogram of number of vortices depinned vs $\max(F_z)$. The width of the histogram bars is the difference in force between heights of successive scans. The arrow on the last blue bin indicates that a single vortex did not move at the largest applied force, as shown in Fig. 2.

motion. For comparison, we normalize previous results by the film thickness and extrapolate to our reduced temperature using the power law $F \propto (1-T/T_c)^{\gamma}$, where γ is an experimentally determined exponent that varies greatly between experiments. The inferred depinning forces are 123,[20] 80,[17] 58,[18] 5,[17] and 0.6 pN/μm.[19] These experiments have motion detection thresholds ranging from a few hundred nanometers to microns, except for Ref. 19, which reports a resolution of $\approx$20–40 nm, achieved with an array of stationary Hall probes.

Our best threshold for vortex motion detection is better than 10 nm and is limited by the signal-to-noise ratio. The characteristic scale for changes in the pinning potential is the coherence length $\xi \approx 10-20$ nm.[17,25] We can therefore detect all vortex depinning events with a quantitative determination of the locally applied depinning force. Imaging the vortices before, during, and after the depinning has great prospects for correlating pinning with topography, for determining the pinning landscape directly, and for studying single-vortex dynamics.

This work was supported by the Packard Foundation, DOE Contract No. DE-AC02–76SF00515, and the (U.S.) Air Force Office of Scientific Research under Contract No. FA50–05–1–0290. We thank Lan Luan for discussions.

[1]D. Larbalestier, A. Gurevich, D. M. Feldmann, and A. Polyanskii, Nature (London) **414**, 368 (2001).
[2]R. M. Scanlan, A. P. Malozemoff, and D. C. Larbalestier, Proc. IEEE **92**, 1639 (2004).
[3]T. Haugan, P. N. Barnes, R. Wheeler, F. Meisenkothen, and M. Sumption, Nature (London) **430**, 867 (2004).
[4]S. Kang, A. Goyal, J. Li, A. A. Gapud, P. M. Martin, L. Heatherly, J. R. Thompson, D. K. Christen, F. A. List, M. Paranthaman, and D. F. Lee, Science **311**, 1911 (2006).
[5]J. E. Villegas, S. Savel'ev, F. Nori, E. M. Gonzalez, J. V. Anguita, R. García, and J. L. Vicent, Science **302**, 1188 (2003).
[6]M. B. Hastings, C. J. Olson Reichhardt, and C. Reichhardt, Phys. Rev. Lett. **90**, 247004 (2003).
[7]M. Berciu, T. G. Rappoport, and J. Boldizsár, Nature (London) **435**, 71 (2005).
[8]C. Weeks, G. Rosenberg, B. Seradjeh, and M. Franz, Nat. Phys. **3**, 796 (2007).
[9]C. J. Olson Reichhardt and M. B. Hastings, Phys. Rev. Lett. **92**, 157002 (2004).
[10]D. R. Nelson, Nature (London) **430**, 839 (2004).
[11]D. R. Nelson, Phys. Rev. Lett. **60**, 1973 (1988).
[12]G. Blatter, M. V. Feigel'man, V. B. Geshkenbein, A. I. Larkin, and V. M. Vinokur, Rev. Mod. Phys. **66**, 1125 (1994).
[13]D. R. Nelson, *Defects and Geometry in Condensed Matter Physics* (Cambridge University Press, Cambridge, 2002).
[14]J. C. Wynn, D. A. Bonn, B. W. Gardner, Y.-J. Lin, R. Liang, W. N. Hardy, J. R. Kirtley, and K. A. Moler, Phys. Rev. Lett. **87**, 197002 (2001).
[15]J. E. Hoffman, E. W. Hudson, K. M. Lang, V. Madhavan, H. Eisaki, S. Uchida, and J. C. Davis, Science **295**, 466 (2002).
[16]Y. Kafri, D. R. Nelson, and A. Polkovnikov, Phys. Rev. B **76**, 144501 (2007).
[17]L. H. Allen and J. H. Claassen, Phys. Rev. B **39**, 2054 (1989).
[18]G. S. Park, C. E. Cunningham, B. Cabrera, and M. E. Huber, Phys. Rev. Lett. **68**, 1920 (1992).
[19]S. T. Stoddart, S. J. Bending, R. E. Somekh, and M. Henini, Supercond. Sci. Technol. **8**, 459 (1995).
[20]M. Breitwisch and D. K. Finnemore, Phys. Rev. B **62**, 671 (2000).
[21]B. W. Gardner, J. C. Wynn, D. A. Bonn, R. Liang, W. N. Hardy, J. R. Kirtley, V. G. Kogan, and K. A. Moler, Appl. Phys. Lett. **80**, 1010 (2002).
[22]A. Moser, H. J. Hug, B. Stiefel, and H.-J. Güntherodt, J. Magn. Magn. Mater. **190**, 114 (1998).
[23]M. Roseman and P. Grütter, Appl. Surf. Sci. **188**, 416 (2002).
[24]Q. Lu, K. Mochizuki, J. T. Markert, and A. de Lozanne, Physica C **371**, 146 (2002).
[25]A. Volodin, K. Temst, Y. Bruynseraede, C. van Haesendonck, M. I. Montero, I. K. Schuller, B. Dam, J. M. Huijbregtse, and R. Griessen, Physica C **369**, 165 (2002).
[26]U. H. Pi, Z. G. Khim, D. H. Kim, A. Schwarz, M. Liebmann, and R. Wiesendanger, Appl. Phys. Lett. **85**, 5307 (2004).
[27]O. M. Auslaender, L. Luan, E. W. J. Straver, J. E. Hoffman, N. C. Koshnick, E. Zeldov, D. A. Bonn, R. Liang, W. N. Hardy, and K. A. Moler, "Mechanics of Individual, Isolated Vortices in a Cuprate Superconductor," Nat. Phys. (in press), preprint at http://arxiv.org/abs/0809.2817.
[28]T. R. Albrecht, P. Grütter, D. Horne, and D. Rugar, J. Appl. Phys. **69**, 668 (1991).
[29]See EPAPS Document No. E-APPLAB-93-029842 for additional discussion. For more information on EPAPS, see http://www.aip.org/pubservs/epaps.html.
[30]E. W. J. Straver, Ph.D. thesis, Stanford University, 2004.
[31]HYPRES, Elmsford, NY.
[32]Masoud Radparvar HYPRES, private communication (April, 2005).
[33]D. M. Eigler and E. K. Schweizer, Nature (London) **344**, 524 (1990).
[34]B. Efron and R. Tibshirani, *An Introduction to the Bootstrap* (Chapman and Hall, New York, 1993).
[35]A. Wadas, O. Fritz, H. J. Hug, and H.-J. Güntherodt, Z. Phys. B: Condens. Matter **88**, 317 (1992).